14th European Signal Processing Conference (EUSIPCO 2006), Florence, Italy, September 4-8, 2006, copyright by EURASIP

ITERATIVE IMAGE DECONVOLUTION USING OVERCOMPLETE REPRESENTATIONS

Caroline Chaux,[1] *Patrick L. Combettes,*[2] *Jean-Christophe Pesquet,*[1] *and Valérie R. Wajs*[2]

[1]Institut Gaspard Monge and UMR 8049, Université de Marne la Vallée, 77454 Marne la Vallée Cedex 2, France
[2]Laboratoire Jacques-Louis Lions – UMR 7598, Université Pierre et Marie Curie – Paris 6, 75005 Paris, France

ABSTRACT

We consider the problem of deconvolving an image with a priori information on its representation in a frame. Our variational approach consists of minimizing the sum of a residual energy and a separable term penalizing each frame coefficient individually. This penalization term may model various properties, in particular sparsity. A general iterative method is proposed and its convergence is established. The novelty of this work is to extend existing methods on two distinct fronts. First, a broad class of convex functions are allowed in the penalization term which, in turn, yields a new class of soft thresholding schemes. Second, while existing results are restricted to orthonormal bases, our algorithmic framework is applicable to much more general overcomplete representations. Numerical simulations are provided.

1. INTRODUCTION

We consider the problem of recovering an image $\bar{x}$ in a real Hilbert space $\mathscr{H}$ from the observation of an image

$$z = T\bar{x} + w, \tag{1}$$

where $T\colon \mathscr{H} \to \mathscr{H}$ is a convolution operator and where $w \in \mathscr{H}$ stands for an additive noise perturbation.

A central concept in image processing is that of a linear representation with respect to a sequence of images $(e_k)_{k\in\mathbb{N}}$ in $\mathscr{H}$. Under suitable assumptions, any image $x \in \mathscr{H}$ can be expanded as $x = \sum_{k\in\mathbb{N}} \xi_k e_k$ and, thereby, represented by a sequence $(\xi_k)_{k\in\mathbb{N}}$ in $\mathbb{R}$. Various operations (coding, compression, transmission, storage, denoising, etc) on x can then be conveniently performed on the sequence of coefficients $(\xi_k)_{k\in\mathbb{N}}$. In early work, the family $(e_k)_{k\in\mathbb{N}}$ was an orthonormal basis, as in standard wavelet representations [15]. More recently, attention has shifted towards more general, overcomplete representations. A convenient tool that captures such representations is the notion of a frame. Recall that a sequence of vectors $(e_k)_{k\in\mathbb{N}}$ in $\mathscr{H}$ is a frame if there exists two constants μ and ν in $]0,+\infty[$ such that

$$(\forall x \in \mathscr{H})\ \ \mu\|x\|^2 \leq \sum_{k\in\mathbb{N}} |\langle x \mid e_k\rangle|^2 \leq \nu\|x\|^2. \tag{2}$$

The associated frame operator is the injective bounded linear operator

$$L\colon \mathscr{H} \to \ell^2(\mathbb{N})\colon x \mapsto (\langle x \mid e_k\rangle)_{k\in\mathbb{N}}, \tag{3}$$

the adjoint of which is the surjective bounded linear operator

$$L^*\colon \ell^2(\mathbb{N}) \to \mathscr{H}\colon (\xi_k)_{k\in\mathbb{N}} \mapsto \sum_{k\in\mathbb{N}} \xi_k e_k. \tag{4}$$

Gabor frames [10, 18] have been used for many years and new frames have been constructed recently, e.g., [13]. When $\mu = \nu$ in (2), the frame is tight. A simple example of a tight frame is the union of m orthonormal bases, in which case $\mu = \nu = m$. For instance, in $\mathscr{H} = \mathrm{L}^2(\mathbb{R}^2)$, a dual-tree wavelet decomposition is the union of two orthonormal wavelet bases [5]. Curvelets [3] constitute an example of a tight frame of $\mathrm{L}^2(\mathbb{R}^2)$. Another common example of a frame is a Riesz basis of $\mathscr{H}$. This corresponds to the case when L is bijective. Then there exists a (unique) biorthogonal basis $(\widetilde{e}_k)_{k\in\mathbb{N}}$ such that, for every $x \in \mathscr{H}$ and $a = (\xi_k)_{k\in\mathbb{N}} \in \ell^2(\mathbb{N})$,

$$x = L^*a \quad \Leftrightarrow \quad (\forall k \in \mathbb{N}) \quad \xi_k = \langle x \mid \widetilde{e}_k\rangle. \tag{5}$$

Examples of Riesz bases of $\mathrm{L}^2(\mathbb{R}^2)$ include biorthogonal bases of compactly supported dyadic wavelets having certain symmetry properties [6]. When $L^{-1} = L^*$, an orthonormal basis is obtained and $(\widetilde{e}_k)_{k\in\mathbb{N}} = (e_k)_{k\in\mathbb{N}}$.

The objective of the present paper is to propose a variational framework to recover an original image $\bar{x}$ given the observation model (1) and some a priori information about the coefficients $(\overline{\xi}_k)_{k\in\mathbb{N}}$ of $\bar{x}$ in a frame $(e_k)_{k\in\mathbb{N}}$, with frame operator L. We seek an image $x = \sum_{k\in\mathbb{N}} \xi_k e_k$, where $a = (\xi_k)_{k\in\mathbb{N}} \in \ell^2(\mathbb{N})$ minimizes the sum of the residual energy $\|Tx - z\|^2/2 = \|TL^*a - z\|^2/2$ and a separable term of the form $\sum_{k\in\mathbb{N}} \phi_k(\xi_k)$, where $(\phi_k)_{k\in\mathbb{N}}$ are convex functions from $\mathbb{R}$ to $]-\infty,+\infty]$ modeling various a priori properties of the ideal coefficients $(\overline{\xi}_k)_{k\in\mathbb{N}}$. More formally, our problem can be stated as follows.

Problem 1 *Let:*

- $T\colon \mathscr{H} \to \mathscr{H}$ *be a nonzero bounded linear operator;*
- $z \in \mathscr{H}$*;*
- $(e_k)_{k\in\mathbb{N}}$ *be a frame of* $\mathscr{H}$ *with frame operator* L*;*
- $(\phi_k)_{k\in\mathbb{N}}$ *be lower semicontinuous convex functions from* $\mathbb{R}$ *to* $]-\infty,+\infty]$ *such that*

$$(\forall k \in \mathbb{N}) \quad \phi_k \geq 0 \quad \textit{and} \quad \phi_k(0) = 0. \tag{6}$$

Set $R = TL^*$*. The objective is to*

$$\underset{a=(\xi_k)_{k\in\mathbb{N}}\in\ell^2(\mathbb{N})}{\text{minimize}} \ \frac{1}{2}\|Ra - z\|^2 + \sum_{k\in\mathbb{N}} \phi_k(\xi_k). \tag{7}$$

When $(e_k)_{k\in\mathbb{N}}$ is an orthonormal basis and $\phi_k = \omega_k|\cdot|^p$ with $p \in [1,2]$ and $\omega_k > 0$, Problem 1 has been treated in [11] and then revisited in a more general algorithmic framework in [9, Section 5.4]. Our analysis will further extend this setting, allowing for more flexible functions such as $\phi_k = \tau_k|\cdot|^{p_k} + \omega_k|\cdot|$, where $\omega_k \geq 0$, $\tau_k \geq 0$, $\omega_k + \tau_k > 0$,

and $p_k \geq 1$. These results are new, even in the context of orthonormal bases.

In Section 2 we provide a brief account of the theory of proximity operators, which play a central rôle in our analysis. In Section 3, we study the class of proximity operators which are soft thresholders, an essential feature in applications with sparsity constraints. Our algorithm is presented in Section 4, along with convergence results. We conclude the paper in Section 5 with numerical simulations.

2. PROXIMITY OPERATORS

Throughout, the underlying image space is a real Hilbert space $\mathscr{H}$ with scalar product $\langle \cdot \,|\, \cdot \rangle$, norm $\|\cdot\|$, and distance d. The indicator function of a nonempty set $C \subset \mathscr{H}$ is

$$\iota_C \colon x \mapsto \begin{cases} 0, & \text{if } x \in C; \\ +\infty, & \text{if } x \notin C \end{cases} \tag{8}$$

and its distance function is $d_C \colon x \mapsto \inf \|C - x\|$. $\Gamma_0(\mathscr{H})$ is the class of all convex lower semicontinuous functions from $\mathscr{H}$ to $]-\infty,+\infty]$ that are not identically $+\infty$. Now let $f \in \Gamma_0(\mathscr{H})$ and $\gamma \in]0,+\infty[$. Then, for every $x \in \mathscr{H}$, the function $y \mapsto f(y) + \|x-y\|^2/2$ achieves its minimum at a unique point denoted by $\operatorname{prox}_f x$. The operator

$$\operatorname{prox}_f \colon \mathscr{H} \to \mathscr{H} \colon x \mapsto \operatorname*{arg\,min}_{y \in \mathscr{H}} f(y) + \frac{1}{2}\|x-y\|^2 \tag{9}$$

is called the proximity operator of f. The reader is referred to [9] for details on these operators.

Example 2 [9] *Let $C \subset \mathscr{H}$ be a nonempty closed convex set and let P_C be the projector onto C. Then* $\operatorname{prox}_{\iota_C} = P_C$ *and* $\operatorname{prox}_{d_C^2/2} = (\operatorname{Id} + P_C)/2$.

A property of proximity operators which is central in the convergence analysis of iterative methods [7], is that they are (firmly) nonexpansive.

Proposition 3 *Let $f \in \Gamma_0(\mathscr{H})$, $x \in \mathscr{H}$, and $y \in \mathscr{H}$. Then*

$$\|\operatorname{prox}_f x - \operatorname{prox}_f y\|^2 + \|(x - \operatorname{prox}_f x) - (y - \operatorname{prox}_f y)\|^2 \leq \|x-y\|^2. \tag{10}$$

Hence, $\|\operatorname{prox}_f x - \operatorname{prox}_f y\| \leq \|x-y\|$.

The following example will be a key tool in the present paper.

Example 4 [9] *Let $(e_k)_{k\in\mathbb{N}}$ be an orthonormal basis of $\mathscr{H}$, let $(\phi_k)_{k\in\mathbb{N}}$ be functions in $\Gamma_0(\mathbb{R})$ such that* (6) *holds and let $f \colon \mathscr{H} \to]-\infty,+\infty] \colon x \mapsto \sum_{k\in\mathbb{N}} \phi_k(\langle x \,|\, e_k\rangle)$. Then $f \in \Gamma_0(\mathscr{H})$ and*

$$(\forall x \in \mathscr{H}) \quad \operatorname{prox}_f x = \sum_{k\in\mathbb{N}} \big(\operatorname{prox}_{\phi_k} \langle x \,|\, e_k\rangle\big) e_k. \tag{11}$$

Example 4 underlines the importance of proximity operators on the Euclidean real line $\mathbb{R}$. Here are a few examples that will be used subsequently.

Example 5 [4] *Let $p \in [1,+\infty[$, let $\omega \in]0,+\infty[$, let*

$$\phi : \mathbb{R} \to]-\infty,+\infty] : \eta \mapsto \omega|\eta|^p, \tag{12}$$

and let $\xi \in \mathscr{H}$. Then $\operatorname{prox}_\phi \xi$ *is given by*

$$\begin{cases} \operatorname{sign}(\xi)\max\{|\xi|-\omega,0\}, & \text{if } p = 1; \\ \xi + \dfrac{4\omega}{3\cdot 2^{1/3}}\Big((\eta-\xi)^{1/3} - (\eta+\xi)^{1/3}\Big), & \\ \quad \text{where } \eta = \sqrt{\xi^2 + 256\omega^3/729}, & \text{if } p = \dfrac{4}{3}; \\ \xi + \dfrac{9\omega^2\operatorname{sign}(\xi)}{8}\left(1 - \sqrt{1 + \dfrac{16|\xi|}{9\omega^2}}\right), & \text{if } p = \dfrac{3}{2}; \\ \xi/(1+2\omega), & \text{if } p = 2; \\ \operatorname{sign}(\xi)\dfrac{\sqrt{1+12\omega|\xi|}-1}{6\omega}, & \text{if } p = 3; \\ \left(\dfrac{\eta+\xi}{8\omega}\right)^{1/3} - \left(\dfrac{\eta-\xi}{8\omega}\right)^{1/3}, & \\ \quad \text{where } \eta = \sqrt{\xi^2 + 1/(27\omega)}, & \text{if } p = 4. \end{cases}$$

3. PROXIMAL SOFT THRESHOLDING

In many applications, the frame $(e_k)_{k\in\mathbb{N}}$ is chosen so that the representation $\bar{x} = \sum_{k\in\mathbb{N}} \overline{\xi}_k e_k$ of the original image is sparse in the sense that "most" of the terms in $(\overline{\xi}_k)_{k\in\mathbb{N}}$ are zero. Intuitively, sparsity can be imposed on a sequence $(\xi_k)_{k\in\mathbb{N}} \in \ell^2(\mathbb{N})$ by setting to zero each coefficient ξ_k such that $|\xi_k| \leq \omega_k$, for some threshold $\omega_k \in]0,+\infty[$.

Definition 6 *A continuous function $p \colon \mathbb{R} \to \mathbb{R}$ is a soft thresholder at level $\omega \in]0,+\infty[$ if $(\forall \xi \in \mathbb{R})$ $p(\xi) = 0 \Leftrightarrow |\xi| \leq \omega$.*

Since we are interested in iterative methods, we cannot use arbitrary soft thresholder and need to restrict ourselves to nonexpansive operators. Many of the soft thresholders employed in denoising, e.g., [2, 16, 17, 19], do not satisfy this property. However, by Proposition 3, soft thresholders which are proximity operators are nonexpansive. For example, for $p = 1$, Example 5 shows that the standard soft thresholding operation (see Fig. 1) [14] results from the proximity operator $\operatorname{prox}_{\omega|\cdot|}$. For this reason, this particular soft thresholder has been used in iterative methods, e.g., [9, 11, 12]. We now characterize *all* proximal soft thresholders.

Proposition 7 [8] *Take $\phi \in \Gamma_0(\mathbb{R})$ such that $\phi(0) = 0$. Then* prox_ϕ *is a soft thresholder at level $\omega \in]0,+\infty[$ if and only if*

$$\phi = \psi + \omega|\cdot|, \quad \text{where } \begin{cases} \psi \in \Gamma_0(\mathbb{R}), \\ \psi \text{ is differentiable at } 0, \\ \psi'(0) = 0. \end{cases} \tag{13}$$

Next, we characterize odd proximal soft thresholders and provide a decomposition rule (see Fig. 1 for illustrations).

Proposition 8 [8] *Let $\phi \in \Gamma_0(\mathbb{R})$. Then* prox_ϕ *is an odd soft thresholder at level $\omega \in]0,+\infty[$ if and only if* (13) *holds with ψ even. In this case, we have* $\operatorname{prox}_\phi = \operatorname{prox}_\psi \circ \operatorname{prox}_{\omega|\cdot|}$.

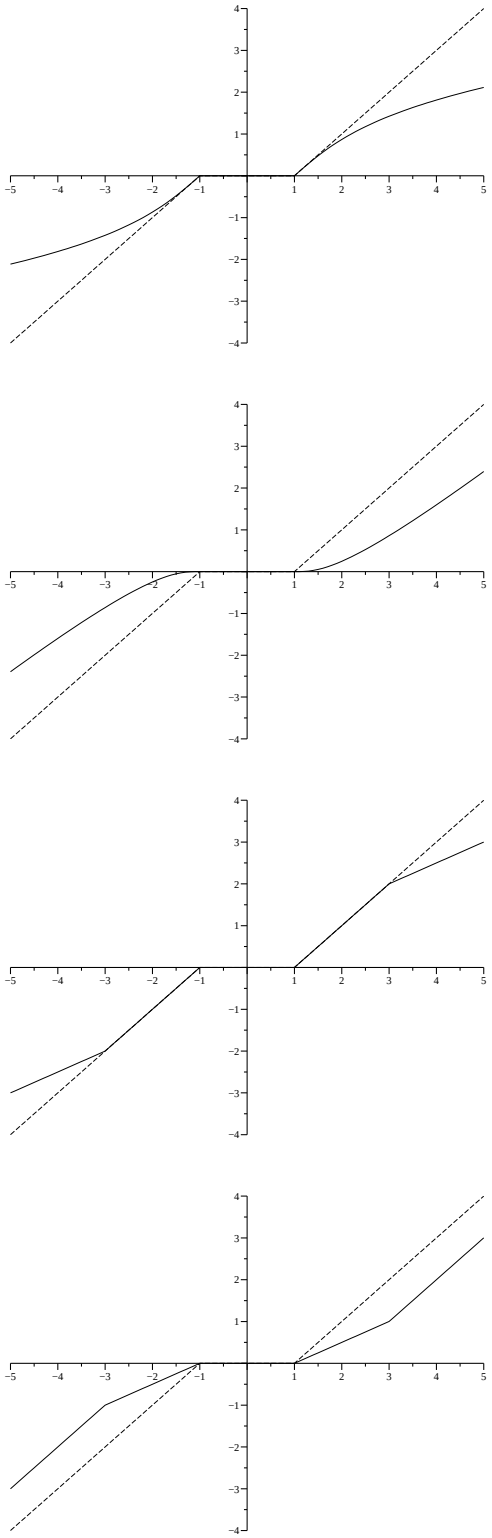

Figure 1: Graph of the proximal thresholder prox_{ϕ}, where ϕ is as in (13) with $\omega = 1$. The dashed line represents the usual soft thresholder obtained with $\psi = 0$. From top to bottom: (a) $\psi = 0.05|\cdot|^4$; (b) $\psi = 0.9|\cdot|^{4/3}$; (c) $\psi = d^2_{[-2,2]}/2$; (d)

$$\psi : \xi \mapsto \begin{cases} \xi^2/2, & \text{if } |\xi| \leq 1; \\ |\xi| - 1/2, & \text{if } |\xi| > 1. \end{cases}$$

4. DECONVOLUTION OVER A FRAME

Let us first address the case when $(e_k)_{k\in\mathbb{N}}$ is an orthonormal basis in Problem 1.

Problem 9 *In Problem 1, suppose that $(e_k)_{k\in\mathbb{N}} = (b_k)_{k\in\mathbb{N}}$ is an orthonormal basis, so that* (7) *reduces to*

$$\underset{x\in\mathscr{H}}{\text{minimize}} \ \frac{1}{2}\|Tx - z\|^2 + \sum_{k\in\mathbb{N}} \phi_k(\langle x \mid b_k\rangle). \tag{14}$$

Proposition 10 [9]

- *Problem 9 possesses at least one solution if there exists $\rho \in]0,+\infty[$ and a function $c\colon [0,+\infty[\to [0,+\infty[$ such that $c(0) = 0$, $\lim_{t\to+\infty} c(t) = +\infty$ and, for every $(\xi_k)_{k\in\mathbb{N}}$ in $\ell^2(\mathbb{N})$ such that $\sum_{k\in\mathbb{N}} |\xi_k|^2 \geq \rho$,*

$$\sum_{k\in\mathbb{N}} \phi_k(\xi_k) \geq c\left(\sum_{k\in\mathbb{N}} |\xi_k|^2\right). \tag{15}$$

- *Problem 9 possesses at most one solution if the functions $(\phi_k)_{k\in\mathbb{N}}$ are strictly convex or if T is injective.*
- *Problem 9 possesses exactly one solution if*
  $(\exists \kappa \in]0,+\infty[)(\forall x \in \mathscr{H})\ \ \|Tx\| \geq \kappa\|x\|$.
- *Let $\gamma \in]0,+\infty[$. Then $x \in \mathscr{H}$ solves Problem 9 if and only if, for every $k \in \mathbb{N}$,*
  $\langle x \mid b_k\rangle = \mathrm{prox}_{\gamma\phi_k} \langle x + \gamma T^*(z - Tx) \mid b_k\rangle$.

Theorem 11 [9] *Suppose that Problem 9 has at least one solution. Let $(\gamma_n)_{n\in\mathbb{N}}$ be a sequence in $]0,+\infty[$ such that $0 < \inf_{n\in\mathbb{N}} \gamma_n \leq \sup_{n\in\mathbb{N}} \gamma_n < 2/\|T\|^2$ and let $(\lambda_n)_{n\in\mathbb{N}}$ be a sequence in $]0,1]$ such that $\inf_{n\in\mathbb{N}} \lambda_n > 0$. For every $n \in \mathbb{N}$, let $(\alpha_{n,k})_{k\in\mathbb{N}}$ be a square-summable sequence and suppose that $\sum_{n\in\mathbb{N}} \sqrt{\sum_{k\in\mathbb{N}} |\alpha_{n,k}|^2} < +\infty$. Fix $x_0 \in \mathscr{H}$ and set*

$$(\forall n \in \mathbb{N})\ \ x_{n+1} = x_n + \lambda_n\left(\sum_{k\in\mathbb{N}} (\pi_{n,k} + \alpha_{n,k}) b_k - x_n\right), \tag{16}$$

where $\pi_{n,k} = \mathrm{prox}_{\gamma_n\phi_k} \langle x_n + \gamma_n(T^*(z - Tx_n)) \mid b_k\rangle$. Then $(x_n)_{n\in\mathbb{N}}$ converges weakly to a solution to Problem 9.

In (16), $\alpha_{n,k}$ stands for some tolerance in the computation of $\mathrm{prox}_{\gamma_n\phi_k} \langle x_n + \gamma_n(T^*(z - Tx_n)) \mid b_k\rangle$. In certain cases, weak convergence can be improved to strong convergence. Thus, the following theorem extends results of [9, 11].

Theorem 12 [8] *Suppose that, for every $k \in \mathbb{N}$,*

$$\phi_k = \tau_k|\cdot|^{p_k} + \omega_k|\cdot|, \tag{17}$$

where $\tau_k \in [0,+\infty[$, $\omega_k \in [0,+\infty[$, $p_k \in]1,+\infty[$, and $p_k \leq 2$ if $\omega_k = 0$. In addition, suppose that $\inf\{\tau_k \mid k \in \mathbb{N},\ \omega_k = 0\} > 0$, $\inf\{\omega_k \mid k \in \mathbb{N},\ \omega_k \neq 0\} > 0$, and $\inf\{p_k \mid k \in \mathbb{N},\ \omega_k = 0\} > 1$. Then Problem 9 has at least one solution and the convergence is strong in Theorem 11.

We now turn to the general setting of Problem 1. First, let us observe that (7) can be rewritten as

$$\underset{a\in\ell^2(\mathbb{N})}{\text{minimize}} \ \frac{1}{2}\|Ra - z\|^2 + \sum_{k\in\mathbb{N}} \phi_k(\langle a \mid b_k\rangle), \tag{18}$$

where $(b_k)_{k\in\mathbb{N}}$ is the canonical basis of $\ell^2(\mathbb{N})$. This formulation now appears as a special case of Problem 9 in the Hilbert space $\ell^2(\mathbb{N})$. Thus, we derive at once from Theorems 11 and 12 the following result.

Proposition 13 [9] *Suppose that Problem 1 has at least one solution. Let $(\gamma_n)_{n\in\mathbb{N}}$ be a sequence in $]0,+\infty[$ such that $0 < \inf_{n\in\mathbb{N}}\gamma_n \leq \sup_{n\in\mathbb{N}}\gamma_n < 2/\|R\|^2$ and let $(\lambda_n)_{n\in\mathbb{N}}$ be a sequence in $]0,1]$ such that $\inf_{n\in\mathbb{N}}\lambda_n > 0$. For every $n\in\mathbb{N}$, let $(\alpha_{n,k})_{k\in\mathbb{N}}$ be a square-summable sequence and suppose that $\sum_{n\in\mathbb{N}}\sqrt{\sum_{k\in\mathbb{N}}|\alpha_{n,k}|^2} < +\infty$. Fix $a_0\in\ell^2(\mathbb{N})$ and set*

$$(\forall n\in\mathbb{N})\quad a_{n+1} = a_n + \lambda_n\Big(\big(\pi_{n,k}+\alpha_{n,k}\big)_{k\in\mathbb{N}} - a_n\Big), \qquad (19)$$

where

$$\pi_{n,k} = \operatorname{prox}_{\gamma_n\phi_k}\langle a_n + \gamma_n(R^*(z-Ra_n)) \mid b_k\rangle. \qquad (20)$$

Then $(a_n)_{n\in\mathbb{N}}$ converges weakly to a solution to Problem 1; the convergence is strong if the conditions of Theorem 12 hold.

5. NUMERICAL EXAMPLES

Frame-based deconvolution. Our goal is to restore the 256×256 satellite SPOT5 image $\bar{x}$ shown in Fig. 2 (top) using Proposition 13. The degraded image z displayed in Fig. 2 (center) is the result of the convolution of $\bar{x}$ with a 7×7 uniform blur and addition of a zero-mean white Gaussian noise w. The convolution operator T satisfies $\|T\| = 1$, the blurred image-to-noise ratio is 30.28 dB, and the relative error is 11.05 dB (the decibel value of the relative error between an image y and $\bar{x}$ is $20\log_{10}(\|\bar{x}\|/\|y-\bar{x}\|)$).

In this restoration example, we use a 2D dual-tree M-band decomposition [5] using the 4-band filter bank of [1, Table VI] over 2 resolution levels. This frame decomposition leads to $\|R\|^2 = 2$ [4] and we take $\gamma_n \equiv 0.995$. In addition, we use $\phi_k = \omega_k|\cdot|^{p_k}$, where $p_k\in\{1,4/3,3/2,2\}$ (see Example 5 for the explicit expression of the proximity operators). For each subband, the parameters (ω_k, p_k) are chosen adaptively.

The restored image shown in Fig. 2 (bottom) has a relative error of 15.14 dB. This leads to a significant improvement not only in terms of relative error (+0.40 dB) but also in visual terms in comparison with deconvolution results obtained with an orthonormal 4-band wavelet basis. Indeed, directions are better preserved and we observe less artifacts.

Deconvolution using proximal soft thresholders. In this second experiment, we employ proximity operators derived from Proposition 8 to restore a 512×512 SPOT5 satellite image. The original image is represented in Fig. 3 (top) and the degraded image z is shown in Fig. 3 (center). Here, T models convolution with a 3×3 uniform blur, $\|T\| = 1$, and w is a zero-mean white Gaussian noise. The blurred image-to-noise ratio is 13.25 dB and the relative error is 12.85 dB.

We consider a decomposition onto a two-dimensional separable orthonormal wavelet basis using the same filter bank as in the previous simulation. In accordance with Theorem 11, we take $\gamma_n \equiv 1.99$ and $\phi_k = \tau_k|\cdot|^{p_k} + \omega_k|\cdot|$. For the approximation coefficients, we set $\omega_k \equiv 0$ and an optimized value of (τ_k, p_k) is chosen with $p_k\in\{4/3,3/2,2\}$ whereas, for detail coefficients, $\omega_k \equiv \omega > 0$ and (τ_k, p_k) is subband-adapted with $p_k\in\{4/3,3/2,2,3,4\}$.

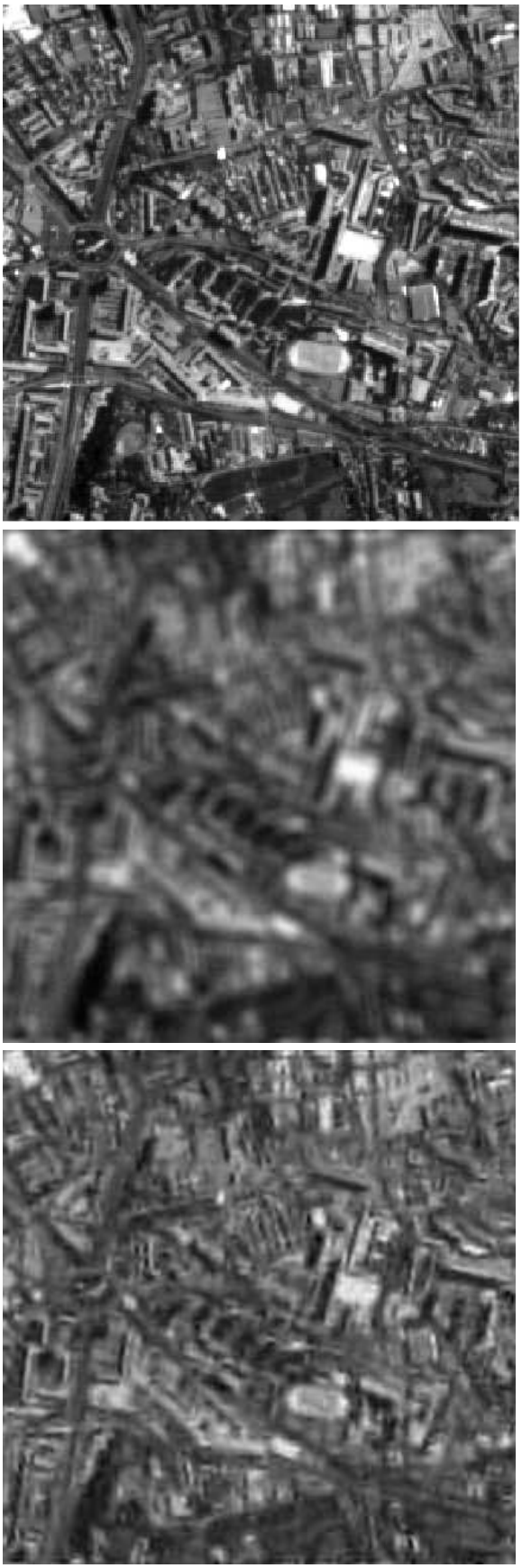

Figure 2: Original image (top), degraded image (center), and restored image (bottom).

Figure 3: Original image (top), degraded image (center), and restored image (bottom).

The restored image displayed in Fig. 3 (bottom) has a relative error of 18.59 dB. Comparatively, in the same conditions, the proximity operators defined in Example 5 lead to a relative error of 18.25 dB.

REFERENCES

[1] O. Alkin and H. Caglar, "Design of efficient *M*-band coders with linear-phase and perfect-reconstruction properties," *IEEE Trans. Signal Process.,* vol. 43, pp. 1579–1590, 1995.

[2] A. Antoniadis, D. Leporini, and J.-C. Pesquet, "Wavelet thresholding for some classes of non-Gaussian noise," *Statist. Neerlandica,* vol. 56, pp. 434–453, 2002.

[3] E. J. Candès and D. L. Donoho, "Recovering edges in ill-posed inverse problems: Optimality of curvelet frames," *Ann. Statist.,* vol. 30, pp. 784–842, 2002.

[4] C. Chaux, P. L. Combettes, J.-C. Pesquet, and V. R. Wajs, "A variational formulation for frame-based image recovery," submitted.

[5] C. Chaux, L. Duval, and J.-C. Pesquet, "Image analysis using a dual-tree *M*-band wavelet transform," *IEEE Trans. Image Process.,* vol. 15, 2006.

[6] A. Cohen, I. Daubechies, and J.-C. Feauveau, "Biorthogonal bases of compactly supported wavelets," *Comm. Pure Appl. Math.,* vol. 45, pp. 485–560, 1992.

[7] P. L. Combettes, "Solving monotone inclusions via compositions of nonexpansive averaged operators," *Optimization,* vol. 53, pp. 475–504, 2004.

[8] P. L. Combettes and J.-C. Pesquet, "A proximal soft thresholding algorithm for minimization over orthonormal bases," submitted.

[9] P. L. Combettes and V. R. Wajs, "Signal recovery by proximal forward-backward splitting," *Multiscale Model. Simul.,* vol. 4, pp. 1168–1200, 2005.

[10] I. Daubechies, *Ten Lectures on Wavelets*. SIAM, Philadelphia, PA, 1992.

[11] I. Daubechies, M. Defrise, and C. De Mol, "An iterative thresholding algorithm for linear inverse problems with a sparsity constraint," *Comm. Pure Appl. Math.,* vol. 57, pp. 1413–1457, 2004.

[12] C. de Mol and M. Defrise, "A note on wavelet-based inversion algorithms," *Contemp. Math.*, vol. 313, pp. 85–96, 2002.

[13] M. N. Do and M. Vetterli, "The contourlet transform: An efficient directional multiresolution image representation," *IEEE Trans. Image Process.,* vol. 14, pp. 2091–2106, 2005.

[14] D. L. Donoho, I. M. Johnstone, G. Kerkyacharian, and D. Picard, "Wavelet shrinkage: Asymptopia?," *J. R. Statist. Soc. B.,* vol. 57, pp. 301–369, 1995.

[15] S. G. Mallat, *A Wavelet Tour of Signal Processing*, 2nd ed. Academic Press, New York, 1999.

[16] G. Steidl, J. Weickert, T. Brox, P. Mrázek, and M. Welk, "On the equivalence of soft wavelet shrinkage, total variation diffusion, total variation regularization, and SIDEs," *SIAM J. Numer. Anal.,* vol. 42, pp. 686–713, 2004.

[17] T. Tao and B. Vidakovic, "Almost everywhere behavior of general wavelet shrinkage operators," *Appl. Comput. Harmon. Anal.,* vol. 9, pp. 72–82, 2000.

[18] R. Tolimieri and M. An, *Time-Frequency Representations.* Birkhäuser, Boston, MA, 1998.

[19] B. Vidakovic, "Nonlinear wavelet shrinkage with Bayes rules and Bayes factors," *J. Amer. Statist. Assoc.,* vol. 93, pp. 173–179, 1998.